Inferring direct directed-information flow from multivariate nonlinear time series

Michael Jachan,[1,2,3,*] Kathrin Henschel,[1,3] Jakob Nawrath,[1,2,4] Ariane Schad,[1] Jens Timmer,[1,3,4,5] and Björn Schelter[1,3,4]
[1]*Center for Data Analysis and Modeling (FDM), University of Freiburg, Eckerstrasse 1, D-79104 Freiburg, Germany*
[2]*Department of Neurology, University Hospital of Freiburg, Breisacher Strasse 64, D-79098 Freiburg, Germany*
[3]*Bernstein Center for Computational Neuroscience (BCCN), University of Freiburg, Hansastrasse 9A, D-79104 Freiburg, Germany*
[4]*Department of Physics, University of Freiburg, Hermann Herder Strasse 3, D-79104 Freiburg, Germany*
[5]*Freiburg Institute for Advanced Studies (FRIAS), University of Freiburg, Albertstrasse 19, D-79104 Freiburg, Germany*
(Received 12 February 2009; published 28 July 2009)

Estimating the functional topology of a network from multivariate observations is an important task in nonlinear dynamics. We introduce the nonparametric partial directed coherence that allows disentanglement of direct and indirect connections and their directions. We illustrate the performance of the nonparametric partial directed coherence by means of a simulation with data from synchronized nonlinear oscillators and apply it to real-world data from a patient suffering from essential tremor.

DOI: 10.1103/PhysRevE.80.011138 PACS number(s): 02.50.Ey, 02.50.Sk, 05.45.Tp

I. INTRODUCTION

First-principles modeling allows gaining of insights into the characteristics of dynamic processes, especially when it comes to understanding complex dynamic networks generated by synchronized self-sustained oscillators [1]. For solving the inverse problem, i.e., inferring the model from measurements, semiparametric and nonparametric techniques developed to infer the network structure based on interacting signals of nonlinear origin have been shown to be very promising. We focus on interactions between coupled nonlinear oscillators that exhibit synchronization, such as phase synchronization [2], lag synchronization, or complete synchronization [3]. To detect the interaction structure of nonlinear systems, measures based on coherence [4], phase, or lag synchronization [3,5,6], or on recurrences [7] are available. Some of these measures can be partialized such that they can distinguish direct and indirect connections but then they cannot resolve the direction of information flow. Methods to detect the direction of coupling in bivariate systems based on phases [8] or on joint recurrence plots [9] have been presented.

Partial directed coherence (PDC), a parametric method that is able to infer directed influences in multivariate—strictly speaking linear—systems, has been widely applied in many fields of time series analysis, i.e., in econometrics, biology, and neuroscience [10–15]. Partial directed coherence analysis is based on the notion of Granger causality, which applies the principle of prediction [10,16–18]. If past observations of a signal $x(t)$ can significantly increase prediction of another signal $y(t)$ given all the information of the remaining possibly multivariate processes, then $x(t)$ is said to Granger cause $y(t)$.

The partial directed coherence, even though it is based on a linear model, has been successfully applied to signals of nonlinear origin [19]. Typically, the parametric partial directed coherence performs well on nonlinear systems only for certain coupling strength. To increase the robustness of partial directed coherence analysis is thus mandatory to guarantee a wide-spread applicability of partial directed coherence to real-world data. In this paper we introduce such a robust extension, a nonparametric measure to infer the causal network structure from multivariate nonlinear possibly chaotic time series: the nonparametric partial directed coherence.

The paper is structured as follows. In the next section the method of nonparametric partial directed coherence is introduced. A significance level based on block bootstrap is derived. The simulation study in Sec. III demonstrates the abilities of nonparametric partial directed coherence when applied to nonlinear synchronizing possibly chaotic systems. An application to human tremor data complements this paper.

II. METHODS

To measure Granger causality, commonly vector autoregressive (VAR) models of order p (VAR[p])

$$\boldsymbol{x}(t) = \sum_{m=1}^{p} \boldsymbol{a}(m)\boldsymbol{x}(t-m) + \boldsymbol{\varepsilon}(t) \tag{1}$$

of the real-valued multivariate stochastic process with D components $\boldsymbol{x}(t)=[x_1(t)x_2(t)\cdots x_D(t)]^T$, where $(\cdot)^T$ denotes vector transposition, are investigated. The $D\times D$ matrices $\boldsymbol{a}(m)$ are the VAR parameter matrices, whose elements $a_{ij}(m)$ govern the interactions from the lagged process components $x_j(t-m)$, $m=1,\ldots,p$ to $x_i(t)$. The noise process $\boldsymbol{\varepsilon}(t)$ is Gaussian distributed with covariance function $\langle \boldsymbol{\varepsilon}(t)\boldsymbol{\varepsilon}^T(t-m)\rangle = \boldsymbol{\Sigma}\delta_{m0}$, where $\Sigma=\langle \boldsymbol{\varepsilon}(t)\boldsymbol{\varepsilon}^T(t)\rangle$ is the noise covariance matrix and δ_{m0} is the Kronecker delta.

The Fourier transform of the VAR coefficients of Eq. (1) $A_{ij}(\omega)=\delta_{ij}-\Sigma_{m=1}^{p}a_{ij}(m)e^{-im\omega}$ leads to the definition of the partial directed coherence

$$\psi_{i\leftarrow j}^{(p)}(\omega) = \frac{|A_{ij}(\omega)|}{\sqrt{\sum_{k=1}^{D}|A_{kj}(\omega)|^2}}, \tag{2}$$

a measure for Granger causality in the frequency domain [12]. It indicates a causal influence from process $x_j(t)$ to $x_i(t)$.

*michael.jachan@gmx.net; www.fdm.uni-freiburg.de/contact/team/jachan

The PDC is normalized as $\psi_{i\leftarrow j}^{(p)}(\omega) \in [0,1]$, the term $\psi_{i\leftarrow i}^{(p)}(\omega)$ quantifies influences on $x_i(t)$, which cannot be explained by other components $x_j(t)$, $j \neq i$. To estimate the PDC, a VAR model is fitted to the observed time series and the VAR parameters are plugged into Eq. (2). Various parameter and order estimators for VAR models have been proposed [20]. For the analysis of the interaction structure of nonlinear processes, the choice of the model order p is not clear; usually a very high order is prescribed to approximate the signal spectra in detail [13,18].

A. Nonparametric PDC

Since partial directed coherence is restricted to parametric VAR processes, the choice of the model order p considerably influences the results obtained. If, for instance, p is chosen too small, wrong causal networks might arise. If the order p is chosen too large, highly fluctuating results might prevent a sensible interpretation of partial directed coherence spectra. Moreover, high model orders usually require large data sets to reliably estimate the VAR parameter matrices. To overcome these limitations we investigate the causal nonparametric model

$$\boldsymbol{x}(t) = \sum_{m=0}^{\infty} \boldsymbol{h}(m)\boldsymbol{\varepsilon}(t-m), \tag{3}$$

characterized by the impulse response $\boldsymbol{h}(m)$, which is normalized to $\boldsymbol{h}(0)=\mathbf{I}_D$. The Fourier transform of the impulse response yields the transfer function, which is given by $\boldsymbol{H}(\omega)=\mathcal{F}\{\boldsymbol{h}(m)\}$. The nonparametric model of Eq. (3) is equivalent to a VAR $[\infty]$ model. Thus $\boldsymbol{H}(\omega)$ can be related to $\boldsymbol{H}^{(p)}(\omega)=\boldsymbol{A}^{-1}(\omega)$ in Eq. (1). The nonparametric PDC (np-PDC) can consequently be defined as

$$\psi_{i\leftarrow j}^{(n)}(\omega) = \frac{|G_{ij}(\omega)|}{\sqrt{\sum_{k=1}^{D} |G_{kj}(\omega)|^2}}, \tag{4}$$

where $G_{ij}(\omega)$ is the (i,j) element of $\boldsymbol{G}(\omega)=\boldsymbol{H}^{-1}(\omega)$. For the nonparametric PDC the same normalization properties as for the parametric PDC of Eq. (2) hold.

Based on Eq. (3) the spectral matrix reads $\boldsymbol{S}(\omega)=\langle \boldsymbol{X}(\omega)\boldsymbol{X}^H(\omega)\rangle = \boldsymbol{H}(\omega)\boldsymbol{\Sigma}\boldsymbol{H}^H(\omega)$. In [16,21,22] an iterative method, the Wilson algorithm, factorizing the spectral matrix by means of a linearization argument and applying Newton's method of obtaining square roots has been proposed. This algorithm computes the unique minimum-phase transfer function $\boldsymbol{H}(\omega)$ given a spectral matrix estimate $\hat{\boldsymbol{S}}(\omega)$ with quadratic convergence. As a spectral estimator we propose to average periodograms of blocks of the observed signal $\boldsymbol{x}(t)$, $t=0,\ldots,N-1$. The signal is cut into nonoverlapping blocks of length N_B, thus integer $K=\lfloor \frac{N}{N_\mathrm{B}} \rfloor$ signal blocks are found. For each block $\boldsymbol{x}^{(k)}(t)$, $k=1,\ldots,K$ the periodogram $\boldsymbol{X}^{(k)}(\omega)[\boldsymbol{X}^{(k)}(\boldsymbol{\omega})]^H$ is computed. The spectral estimate is obtained by averaging the block periodograms

$$\hat{\boldsymbol{S}}(\omega) = \frac{1}{K}\sum_{k=1}^{K} \boldsymbol{X}^{(k)}(\omega)[\boldsymbol{X}^{(k)}(\omega)]^H. \tag{5}$$

This block-averaging spectral estimator reduces the spectral resolution, which could be obtained by the smoothing method [23]. However, this decreased resolution enables a rigorous statistical assessment of the results as presented in the next section. Below we also discuss how to estimate the optimal block length, which guarantees sufficient resolution and thus, maximum stability based on the data itself.

B. Significance level

To derive a significance level for the proposed method, a block-bootstrap approach [24,25] is introduced here. In order to generate a set of M resampled spectral matrices, the individual blocks of the ith component of $\boldsymbol{X}(\omega)$, which are $\{X_i^{(1)}(\omega),\ldots,X_i^{(k)}(\omega),\ldots,X_i^{(K)}(\omega)\}$, are shuffled with replacement for all $i=1,\ldots,D$. Using this procedure, the interaction structure is destroyed but the other signal characteristics are preserved. Repeating this procedure M times leads to M spectral matrices. Thereby, M estimates for the nonparametric PDC under the null hypothesis of absent coupling can be computed. The $(1-\alpha)$ quantile of the distribution of Eq. (4) generated out of the M samples, which are consistent with the null hypothesis, serves as the significance level.

For univariate processes $x(t)$, a method to estimate the optimal block length based on the decay of the autocorrelation function (ACF) of $x(t)$ has been derived [26]. Fitting an exponential law ϕ^τ to the ACF $r(\tau)$, the optimal block length for nonoverlapping blocks is given by

$$N_\mathrm{B} = \left[4N\left(\frac{\phi}{1-\phi} + \frac{\phi^2}{(1-\phi)^2} \right)^2 \left(1 + \frac{2\phi}{1-\phi} \right)^{-2} \right]^{1/3}. \tag{6}$$

Since we are interested in interactions between processes here, we extend this approach to the correlation matrix of $\boldsymbol{x}(t)$ by fitting $\phi^{(\tau-\tau_0)}$ to all ACFs and normalized cross-correlation functions. The maximum of N_B derived based on the full correlation matrix of $\boldsymbol{x}(t)$ is considered the optimal block length.

Please note that this optimal block length is estimated to be purely data driven by exploiting the decay properties of the autocorrelation and cross-correlation functions. Thus, also the spectral resolution is determined by this optimal block length. Although one could in principle increase the resolution in the frequency domain by increasing the block length compared to the optimal one, this procedure would hamper the statistics derived based on this shorter block length. Confidence would be based on correlated data, which would render them useless. If the statistical stability should be increased, increasing the recording length of the data is the only apt solution.

III. SIMULATIONS

The performance of smoothed partial directed coherence and the validity of the significance level are assessed by power and coverage analysis for simulated dynamical processes. The power of a statistical test quantifies the ability to

detect a violation of the null hypothesis while the coverage controls the fraction of false positive errors, i.e., α errors. We present two stochastically driven coupled nonlinear systems for which we analyze power and coverage of the npPDC and its significance level.

The first process is a two-dimensional stochastically driven van-der-Pol oscillator

$$\ddot{x}_1 = \mu(1 - x_1^2)\dot{x}_1 - \omega_1^2 x_1 + \varepsilon_1, \tag{7}$$

$$\ddot{x}_2 = \mu(1 - x_2^2)\dot{x}_2 - \omega_2^2 x_2 + \varepsilon_2 + \gamma(x_1 - x_2), \tag{8}$$

with $N=50\,000$, where $x_1(t)$ drives $x_2(t)$ with a varying diffusive coupling strength given by γ. The van-der-Pol differential equations describe limit cycle oscillators governed by the nonlinearity parameter $\mu=5$ with frequencies $\omega_1=2\pi$ and $\omega_2=1.03\omega_1$. The system is driven by Gaussian white noise $\varepsilon_{1,2}$ with zero mean and variance of two. The coupling strength γ is varied between zero and three.

Further, the x components of two coupled stochastic Rössler oscillators with $N=50\,000$ defined by

$$\begin{bmatrix} \dot{x}_i \\ \dot{y}_i \\ \dot{z}_i \end{bmatrix} = \begin{bmatrix} -\omega_i y_i - z_i + \sum_{j \neq i} \gamma_{i,j}(x_j - x_i) + \varepsilon_i \\ \omega_i x_i + a y_i \\ b + (x_i - c) z_i \end{bmatrix}, \tag{9}$$

$i,j=1,2$, have been analyzed. The parameters that govern chaotic behavior are set to $a=0.15$, $b=0.2$, and $c=10$. The respective frequencies are $\omega_1=2\pi$, $\omega_2=1.03\omega_1$, and the driving white Gaussian white-noise processes $\varepsilon_{1,2}$ are zero mean with variance of four to obtain satisfactory mixing properties [27]. The coupling parameter $\gamma=\gamma_{2,1}$ is varied between 0 and 0.10 while $\gamma_{1,2}=0$.

For these two systems we simulated 100 realizations for each chosen value of γ. Numeric integration of the nonlinear stochastic systems has been performed by an Euler method with integration step of 0.001 and a sampling step of 0.1. At the frequency $\omega_0=2\pi$ we evaluated the nonparametric PDC and tested it for significance. A significant value of $\psi^{(n)}_{2\leftarrow 1}(\omega_0)$ indicates a true positive while a significant value of $\psi^{(n)}_{1\leftarrow 2}(\omega_0)$ is a false positive. In Fig. 1 the power curve, i.e., the percentage of detected connections from $x_1(t)$ to $x_2(t)$ (bold line) as well as from $x_2(t)$ to $x_1(t)$ (thin line) for varying coupling strength is shown.

The coverage of the bootstrap is shown for zero coupling, where connections in both directions are detected in not more cases than expected for the significance level of 5%. The power is verified for a certain minimal-coupling strength where the nonparametric PDC detects the connection $x_1(t)$ to $x_2(t)$ almost surely for both systems. The connection $x_2(t)$ to $x_1(t)$ is detected in $\leq 5\%$ of all cases regardless of the coupling strength, which is again expected for the 5% significance level.

To characterize the synchronization regimes of the oscillators in more detail, we analyzed both systems for synchronization of phases by the mean phase coherence (MPC) [2] and for lag synchronization by the lag synchronization index [3]. For the noise-free van-der-Pol system lag synchronization starts for a coupling value of $\gamma_L \approx 0.3$, while the onset of complete synchronization is at $\gamma_C \approx 2.1$. For the noise-free Rössler system phase synchronization starts at $\gamma_P \approx 0.06$ and the onset of lag synchronization is at $\gamma_L \approx 0.20$. For the noisy van-der-Pol system, the npPDC can correctly find the interaction up to the maximum coupling value of $\gamma_{max}=3$, for which the average MPC is 0.7. For the noisy Rössler system the npPDC provides correct results up to $\gamma_{max}=0.1$, which corresponds to an average MPC of 0.75. At γ_{max}, both the noise-free and the noiseless systems are in lag synchronization. Thus, for both systems, applicability of the npPDC is provided for a coupling strength corresponding to a coupling regime that can reach beyond the onset of phase synchronization or even to moderate lag synchronization. If however the coupling is higher than γ_{max}, the coupling is expectedly too strong and the npPDC is significant in both directions. This is a well-known issue and has been addressed by several authors. See for instance [19].

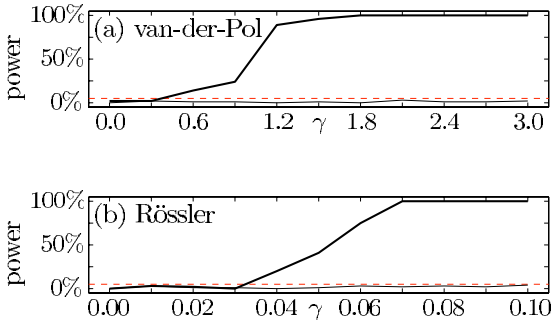

FIG. 1. (Color online) Percentage of detections for (a) van-der-Pol oscillators, and (b) Rössler oscillators. Bold line: $x_1(t)$ to $x_2(t)$ (true positives), thin line: $x_2(t)$ to $x_1(t)$ (false positives). With increasing coupling strength the connection $x_1(t)$ to $x_2(t)$ is detected more often but the absent connection $x_2(t)$ to $x_1(t)$ is detected with an error level of 5%, which corresponds to the significance level (indicated by a gray dashed line).

To investigate the performance of the nonparametric PDC and its significance level, a stochastically driven Rössler processes with four components, $N=100\,000$, and $a=0.15$, $b=0.2$, $c=10$ is simulated [cf. Eq. (9)]. The frequencies are $\omega_1=2\pi$, $\omega_2=1.02\omega_1$, $\omega_3=1.04\omega_1$, and $\omega_4=1.06\omega_1$, and the driving noise processes are with variance of four. The coupling parameters are $\gamma_{1,2}=0.05$, $\gamma_{2,1}=0.05$, $\gamma_{4,2}=0.05$, $\gamma_{3,4}=0.05$, and $\gamma_{2,3}=0.05$, and all others are zero. This model exhibits a bidirectional interaction between $x_1(t)$ and $x_2(t)$, and a loop of unidirectional interactions $x_2(t)$ to $x_4(t)$, $x_4(t)$ to $x_3(t)$, and $x_3(t)$ to $x_2(t)$. The optimal block length is $N_B=4000$ such that 25 blocks resulted. In Fig. 2 the nonparametric PDC estimates are shown. The simulated interaction structure has correctly been revealed by the nonparametric PDC together with the significance level.

IV. APPLICATION TO TREMOR DATA

To show the applicability of the nonparametric PDC together with its significance level to real-world data, we present an analysis of the causality structure of a recording from a patient suffering from essential tremor. This common movement disorder is characterized by a postural tremor of

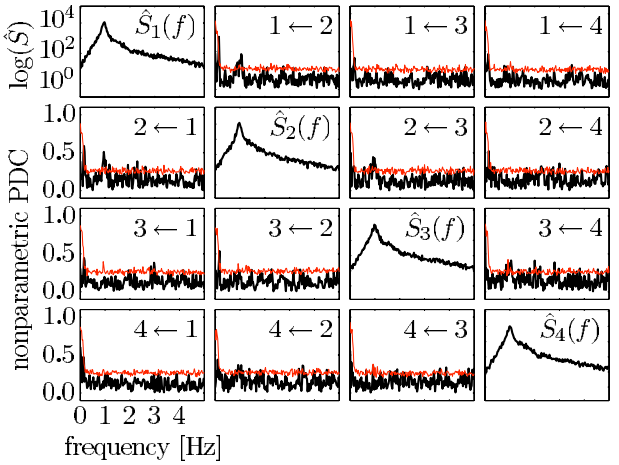

FIG. 2. (Color online) Nonparametric PDC of the Rössler system. Gray lines indicate bootstrapped significance levels. The connections $1 \leftarrow 2$, $2 \leftarrow 1$, $4 \leftarrow 2$, $3 \leftarrow 4$, and $2 \leftarrow 3$ are significant. The spectra $\hat{S}$ are displayed in arbitrary units.

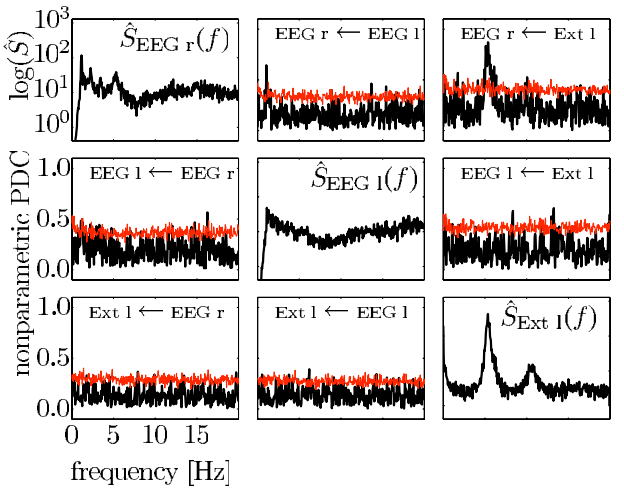

FIG. 4. (Color online) Nonparametric PDC of the tremor data set and the block-averaged periodograms in logarithmic scale. It shows a connection from the left extensor to the right EEG, especially at the tremor frequency of 5 Hz. At 10 Hz, there is a first harmonic of the tremor EMG indicating a nonlinear signal generation mechanism.

the arms and possibly other body parts. The trembling frequency usually is between 4 and 8 Hz.

Tremor-correlated activity has been found in cortical structures [28], where it was shown that the electromyogram (EMG) of flexor and extensor muscles of the trembling hand is coherent to the electroencephalogram (EEG) of the contralateral sensori-motor cortex at the tremor frequency. It remains an open question whether the cortex imposes its oscillatory behavior onto the muscles or whether the muscles send feedback to the cortex. This question can be addressed using the nonparametric PDC.

To this aim, on-scalp EEG has been recorded together with the EMG of the extensor and flexor muscles. The EEG over the right sensori-motor cortex, the EEG over the left sensori-motor cortex, and the EMG from the wrist extensor of the left hand are analyzed with a sampling frequency of 100 Hz. For a data segment with $N=30\,000$, the EMG has been rectified, filtered, and the mean has been subtracted [28].

Figure 3 shows the traces of the signal and in Fig. 4 the nonparametric PDC including the autospectra on the main diagonal are shown. Connections from the left extensor to the right sensori-motor cortex at the tremor frequency of 5 Hz are detected, whereas the direction from left extensor to the left sensori-motor cortex does not show a significant interaction at the tremor frequency. The presence of a harmonic component in the tremor signal indicates a nonlinear signal generation mechanism of second order. It can be concluded that the measured data display the feedback of the muscle to the motor cortex.

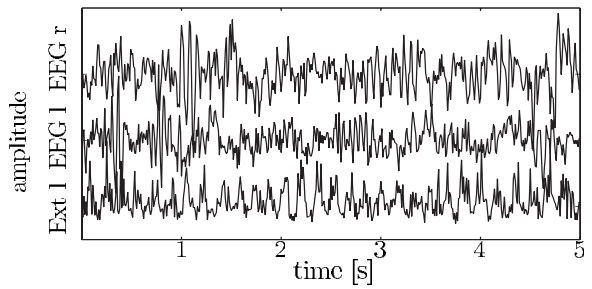

FIG. 3. Tremor data, zoomed segment of 5 s. The first and second traces are the EEG signals while the third trace is the rectified and filtered EMG. The traces are rescaled to equalize their variances and are depicted in arbitrary units.

For the results depicted in Fig. 4 the variances of the three signals were equalized to one to increase numeric stability. We did not observe different results for cases where the variances differed by one order of magnitude.

V. DISCUSSION AND CONCLUSION

In summary, we introduced an alternative approach for the inference of frequency-resolved direct directed interaction structures based on nonparametric spectral estimation. A major advantage of the proposed significance level is that it provides information about its applicability. Imagine that the estimated minimal block length N_B is of the order of the available data points N, then the proposed block-averaging procedure is not applicable. This indicates that the amount of data is too small to reliably estimate the interaction structure of the network. In this case, it is also possible to use the block-length estimator [Eq. (6)] to estimate the minimal recording length needed since as a rule of thumb the number of blocks K should at least be ten to get a reliable estimate. The proposed interaction measure can also be readily applied to point process data or hybrids of time series and point processes since only differences in the Fourier transform for both types of processes have to be taken into account. The nonparametric partial directed coherence can successfully

infer direct directed interactions from multivariate nonlinear possibly chaotic dynamical systems.

ACKNOWLEDGMENT

This work was supported by the German Federal Ministry of Education and Research (Contract No. 01GQ0420), the German Science Foundation (Contracts No. Ti315/4-2 and No. He1949/1-1), and the European Union (EPILEPSIAE, Grant No. 211713). This work was supported by the Excellence Initiative of the German Federal and State Governments. The authors thank B. Guschlbauer, F. Amtage, B. Hellwig, and C. H. Lücking for providing the tremor data and for fruitful discussions.

[1] A. S. Pikovsky, M. G. Rosenblum, and J. Kurths, *Synchronization–A Universal Concept in Nonlinear Sciences* (Cambridge University Press, Cambridge, 2001).
[2] F. Mormann, K. Lehnertz, P. David, and C. E. Elger, Physica D **144**, 358 (2000).
[3] M. G. Rosenblum, A. S. Pikovsky, and J. Kurths, Phys. Rev. Lett. **78**, 4193 (1997).
[4] M. Winterhalder, B. Schelter, W. Hesse, K. Schwab, L. Leistritz, D. Klan, R. Bauer, J. Timmer, and H. Witte, Signal Process. **85**, 2137 (2005).
[5] M. G. Rosenblum, A. S. Pikovsky, and J. Kurths, Phys. Rev. Lett. **76**, 1804 (1996).
[6] B. Schelter, M. Winterhalder, R. Dahlhaus, J. Kurths, and J. Timmer, Phys. Rev. Lett. **96**, 208103 (2006).
[7] N. Marwan, M. C. Romano, M. Thiel, and J. Kurths, Phys. Rep. **438**, 237 (2007).
[8] M. G. Rosenblum and A. S. Pikovsky, Phys. Rev. E **64**, 045202(R) (2001).
[9] M. C. Romano, M. Thiel, J. Kurths, and C. Grebogi, Phys. Rev. E **76**, 036211 (2007).
[10] J. Granger, Econometrica **37**, 424 (1969).
[11] M. J. Kamiński and K. J. Blinowska, Biol. Cybern. **65**, 203 (1991).
[12] L. A. Baccalá and K. Sameshima, Biol. Cybern. **84**, 463 (2001).
[13] B. Schelter, M. Winterhalder, M. Eichler, M. Peifer, B. Hellwig, B. Guschlbauer, C. Lücking, R. Dahlhaus, and J. Timmer, J. Neurosci. Methods **152**, 210 (2006).
[14] Z. Zhou, Y. Chen, M. Ding, P. Wright, Z. Lu, and Y. Liu, Hum. Brain Mapp. **30**, 2197 (2009).
[15] H. Witte, M. Ungureanu, C. Ligges, D. Hemmelmann, T. Wüstenberg, J. Reichenbach, L. Astolfi, F. Babiloni, and L. Leistritz, Methods Inf. Med. **48**, 18 (2009).
[16] M. Dhamala, G. Rangarajan, and M. Ding, Phys. Rev. Lett. **100**, 018701 (2008).
[17] M. Dhamala, G. Rangarajan, and M. Ding, Neuroimage **41**, 354 (2008).
[18] M. Winterhalder, B. Schelter, and J. Timmer, Int. J. Bifurcation Chaos Appl. Sci. Eng. **17**, 3735 (2007).
[19] D. Smirnov, B. Schelter, M. Winterhalder, and J. Timmer, Chaos **17**, 013111 (2007).
[20] H. Lütkepohl, *Introduction to Multiple Time Series Analysis* (Springer, New York, 1993).
[21] G. Tunnicliffe Wilson, SIAM J. Appl. Math. **23**, 420 (1972).
[22] A. H. Sayed and T. Kailath, Numer. Linear Algebra Appl. **8**, 467 (2001).
[23] P. Bloomfield, *Fourier Analysis of Time Series: An Introduction* (John Wiley & Sons, New York, 1976).
[24] B. Efron, Ann. Stat. **7**, 1 (1979).
[25] E. Mammen, in *When Does Bootstrap Work? Asymptotic Results and Simulations*, Lecture Notes in Statistics No. 77 (Springer, New York, 1992).
[26] M. Peifer, B. Schelter, B. Guschlbauer, B. Hellwig, C. Lücking, and J. Timmer, Biom. J. **47**, 346 (2005).
[27] M. Peifer, B. Schelter, M. Winterhalder, and J. Timmer, Phys. Rev. E **72**, 026213 (2005).
[28] B. Hellwig, S. Häußler, B. Schelter, M. Lauk, B. Guschlbauer, J. Timmer, and C. Lücking, Lancet **357**, 519 (2001).